Published in final edited form as:
Dev Dyn. 2008 October ; 237(10): 2918–2925. doi:10.1002/dvdy.21720.

VEGF-mediated fusion in the generation of uniluminal vascular spheroids

Carmine Gentile[1,*], **Paul A. Fleming**[1,*], **Vladimir Mironov**[1], **Kelley M. Argraves**[1], **W. Scott Argraves**[1], and **Christopher J. Drake**[1,2]
[1]Department of Cell Biology and Anatomy, Medical University of South Carolina, Charleston, SC 29425

Abstract

Embryonic mouse allantoic tissue (E8.5) was cultured in hanging drops to generate a three-dimensional vascular micro-tissue. The resulting tissue spheroids had an inner network of small diameter PECAM-1-positive vessels and an outer layer of cells expressing SMαA, SM22-α, and SM-MHC. In a subsequent phase of culture, the fusion-promoting activity of VEGF was used to transform the inner network of small diameter endothelial tubes into a contiguous layer of cells expressing PECAM-1, CD34 and VE-cadherin that circumscribed a central lumen-like cavity. The blood vessel-like character of the VEGF-treated spheroids was further demonstrated by their physiologically relevant vasodilatory and contractile responses, including contraction induced by KCl and relaxation stimulated by high-density lipoproteins and acetylcholine-induced nitric oxide production.

Keywords

VEGF; vascular fusion; blood vessel; micro-tissue; spheroid; endothelial cell; smooth muscle cell

Introduction

Recent efforts to elucidate the molecular regulation of vascular morphogenesis have focused on the generation of three-dimensional micro-tissues that allow interactions between endothelial cells (ECs) and vascular smooth muscle cells (SMCs) to be investigated. For example, Korff et al. (2001), using human umbilical vein ECs (HUVECs) and human umbilical artery smooth muscle cells (HUASMCs), have generated tissue spheroids in carboxymethylcellulose that were characterized by an outer layer of ECs which surrounded an inner core of SMCs. These spheroids have been used to study paracrine interactions between ECs and mural cells (e.g., SMCs) that mediate vascular endothelial cell growth factor (VEGF) signaling (Korff et al., 2001), and most recently, to investigate Tie-2/angiopoietin-2 signaling (Scharpfenecker et al., 2005). Using the same cell types, Kelm et al. (2005) generated spheroids in hanging drop culture characterized by an outer layer of SMCs surrounding an inner mass of ECs that lacked lumens. Using these spheroids, Kelm and colleagues investigated VEGF production and its effects on blood vessel formation.

Here we sought to generate a spheroid that more closely recapitulated the features of a blood vessel. Specifically, we were interested in generating a spheroid with an outer layer of SMCs surrounding a single inner endothelium with a central lumen. Using exogenous VEGF as a

[2]Address correspondences to: Christopher J. Drake, Ph.D. Department of Cell Biology and Anatomy Medical University of South Carolina Charleston, SC 29425 Tel.: (843) 792-1692 Fax: (843) 792-0664 Email: drakec@musc.edu.
[*]These authors contributed equally to this work.

means of promoting the fusion of blood vessels (Drake and Little, 1995; Drake and Fleming, 2000; Argraves et al., 2002; Dor et al., 2002; Dominguez et al., 2007), we report the generation of mouse allantoic-derived vascular spheroids that are characterized by an outer layer of SMCs (i.e., smooth muscle α-actin [SMαA], SM22-α, smooth muscle myosin II heavy chain [SM-MHC] expressing cells) surrounding an inner endothelium (i.e., PECAM-1, CD34, VE-cadherin expressing cells) defining a central lumen like cavity. Further, we show that these vascular spheroids exhibit physiologically relevant vasodilatory and contractile responses.

Results

Generation of vascular spheroids from mouse allantois tissue

When allantoides isolated from E8.5 mouse embryos (Fig. 1A) were cultured in a hanging drop for 18 h, they took on a spherical shape (Fig. 1B), with a mean outer diameter of 440.5 μm ± 39.08 (n = 17). Analysis of laser scanning confocal microscopy (LSCM) z-series projections showed that the spheroids were comprised of an outer layer of SMαA positive (Fig. 1C, red), SM22-α positive (*data not shown*), and smooth muscle myosin positive (*data not shown*) cells that surrounded an inner three-dimensional capillary-like network of PECAM-1 positive (Fig. 1C, *green*), CD34 positive (*data not shown*) cells. Examination of three-micron physical sections of the spheroids (Fig. 1D) revealed that the PECAM-1-positive cells (*green*) surrounded immunonegative areas that may represent either vascular lumens or extravascular spaces that separate PECAM-1-positive cells.

Exogenous VEGF promotes the fusion of spheroid blood vessels

Given the established ability of VEGF to promote the fusion of blood vessels to form vessels of increased diameter (Drake and Little, 1995; Argraves et al., 2002; Dor et al., 2002; Dominguez et al., 2007), the effect of exogenously added VEGF on the blood vessels of allantoic spheroids was investigated. Analysis of a LSCM z-series acquired from a VEGF-treated spheroid that was immunolabeled with antibodies to PECAM-1 and SMαA showed that VEGF profoundly affected the EC component of the spheroids. Rather than a network of luminized PECAM-1-positive vessels occupying the center of the spheroid, as was seen in the untreated spheroids (Fig. 1D) analysis of optical section(s) acquired from VEGF-treated spheroids showed that treated spheroids were uniluminal; having a single inner layer of PECAM-1 (Fig. 2A, *green*) expressing ECs that circumscribed a single large central immuno-negative area. Conventional fluorescence microscopic analysis of 3 μm sections of paraffin embedded VEGF-treated spheroids immunolabeled with antibodies to PECAM-1 (Fig. 2B, *green*) and SMαA (Fig. 2B, *red*) confirmed the overall morphological effects of VEGF, and showed that the endothelium, while continuous, was not uniform. In some areas the endothelial cells appeared as a simple squamous layer (Fig. 2B, *asterisk*) whereas in other areas the endothelium was stratified, with PECAM-1 positive projections evident (Fig. 2B, *arrowheads*).

The central space of VEGF-treated allantoic spheroids is analogous to a vascular lumen

Since the lumen of a normal blood vessel is circumscribed by an endothelium, we next investigated whether the PECAM-1 expressing ECs in VEGF treated spheroids expressed the EC specific cell-cell junction protein, VE-cadherin. As seen in Figure 3A, LSCM analysis of VEGF treated spheroids immunolabeled using antibodies to VE-cadherin (*green*) and SMαA (*red*) revealed that PECAM-1 positive ECs that surrounded the central space also expressed VE-cadherin. While the above observations suggested that the central space is lined by a vascular endothelium it remained unclear whether the endothelium was contiguous and thus able to act as barrier. To evaluate this, 15-20 nm quantum dot nanocrystals (Qdots) were injected into the central cavity of the spheroid. *In vivo* studies have shown that Qdots injected into the circulatory system of zebrafish are retained within blood vessels (Rieger et al.,

2005). As shown in Figure 3C, Qdots injected into spheroids (Fig. 3B) filled the entire central space. Further, observations of injected spheroids showed that the Qdots did not leak out of the central space into the surrounding SMαA-positive cell layer (*data not shown*). These findings, in conjunction with the finding that the ECs lining the cavity express VE-cadherin, suggest that the cavity is lined by a contiguous endothelium and is, therefore, analogous to the lumen of a blood vessel.

Cells forming the outer layer of the spheroid express SMαA, SM22-α and SM-MHC

Additional immunohistological analysis was performed to determine whether cells of the outer layer of the VEGF-treated spheroids expressed SMC proteins in addition to SMαA (Fig. 4A). As shown in Figure 4C and D, the outer layer of cells expressed both SM22-α and SM-MHC, two well-established SMC proteins (Duband et al., 1993;Miano et al., 1994;Li et al., 1996;Madsen et al., 1998). Further, high magnification LSCM analysis of the SMαA labeled cells showed that the actin proteins were organized in filamentous networks (Fig. 4B), suggestive of a functional contractile apparatus.

Cells of the outer SMC layer are closely associated with cells of the inner endothelial layer

Initial immunohistological analysis of VEGF-treated spheroids suggested that SMαA-positive and PECAM-1-positive cell layers were separated by other non-immunoreactive cells (Fig. 2). However, high magnification LSCM analysis of VEGF-treated spheroids immunolabeled with SM22-α and PECAM-1 showed that SM22-α-positive cells (SMCs) extend from the outer surface of the spheroid to the inner endothelial layer (Fig. 5). The cytoplasmic immunostaining achieved with SM22-α antibody highlighted the close interaction between the SM22-α-positive cells and ECs (Fig. 5C, *arrows*).

VEGF-treated spheroids respond to agents that regulate vascular tone

To evaluate whether the VEGF-treated spheroids exhibited physiologically relevant vasodilatory and contractile responses, the spheroids were treated with well-described regulators of vascular tone. First, spheroids were treated with KCl, a mediator of SMC contraction (Dora et al., 1997; Hadoke et al., 2001; Ross et al., 2006). This treatment resulted in an overall reduction in spheroid diameter. Within 15 minutes of KCl exposure, the spheroids reached 50% of the maximal contraction, which was achieved after 1 hour of treatment (Fig. 6A). Next, we evaluated the capacity of the EC component of spheroids to modulate the activity of the SMC component. To do this, spheroids that had been pre-contracted with KCl were treated with acetylcholine (ACh), a vasorelaxant. As seen in Figure 6B, the spheroid diameter of pre-contracted spheroids increased in response to ACh. To evaluate the extent to which the ACh-mediated relaxation of the spheroids was attributable to nitric oxide (NO), an EC-generated mediator of vascular SMC relaxation (Furchgott and Zawadzki, 1980), pre-contracted spheroids were exposed to an inhibitor of endothelial cell NO production, L-NAME. As seen in Figure 6C, L-NAME inhibited the ACh-mediated relaxation of the spheroids.

Another important physiological mediator of vascular tone is sphingosine-1-phosphate (S1P), a lysophospholipid carried in the blood by HDL (Murata et al., 2000). Using aortic ring-based assays to evaluate vasorelaxation, Nofer et al., (2004) have demonstrated that HDL promotes vasorelaxation via signaling through the S1P receptor, S1P3. To determine whether spheroids exhibit a similar vasodilatory response we evaluated the response of pre-contracted spheroids from wild-type and S1P3-deficient mice to HDL. As shown in Figure 7, KCl-contracted spheroids from both wild-type and S1P3 nulls relaxed in response to HDL treatment. However, the magnitude of the relaxation observed in S1P3-deficient spheroids was less (~50%) than that of wild-type spheroids. The observed HDL effects were similar to those observed using aortic rings in which S1P3-deficient aortic rings relaxed 57% that of wild-type in response to HDL (Nofer et al., 2004).

Discussion

Here we describe the development of vascular micro-tissues (vascular spheroids) that are characterized by an outer layer of SMαA-, SM22-α-, and SM MHC-positive cells and an inner cavity lined by PECAM-1-, CD34- and VE-cadherin-positive cells. ECs lining the cavity exhibit properties of a vascular endothelium as evidenced by VE-cadherin expression and the fact that injected Q-dots are retained with in the cavity. The fact that Qdots, which have a diameter similar to that of low-density lipoprotein particles (Rohrer et al., 2006; Teerlink and Scheffer, 2007), do not leak from the lumen-like cavity into the subendothelial space may be an indication that the endothelium of the vascular spheroids displays physiological macromolecular barrier function.

The finding that spheroids derived from E8.5 allantoides generate SMCs is of interest considering that SMCs are not present in the allantois *in vivo* at E8.5. It is possible that the SMCs arose through differentiation of allantoic mesenchymal cells (Downs et al., 2001). It is also possible that the SMCs arose either directly from Flk1 positive cells (Yamashita et al., 2000) or via a transdifferentiation of endothelial cells (Frid et al., 2002; Ishisaki et al., 2003). Whatever the progenitor may be, it appears that our culture conditions potentate the differentiation of SMCs in explanted allantoides.

Our studies also demonstrated that ECs and SMCs of vascular spheroids are capable of physiologically relevant cell-cell signaling. This conclusion is supported by evidence that ECs were able to mediate the relaxation of the smooth muscle layer via ACh-induced NO production. The fact that the ACh-mediated relaxation of vascular spheroidal SMCs was not completely inhibited by L-NAME suggested an eNOS-independent component. This interpretation is consistent with findings from studies of mice deficient in eNOS, which also revealed an eNOS independent vasodilatory mechanism (Chataigneau et al., 1999). Similar to what we observed, Chataigneau et al. (1999) found that ACh-induced SMC relaxation of mesenteric arteries was only partially blocked by L-NAME. The eNOS-independent relaxation process in these arteries appeared to involve a product of cyclo-oxygenase (Chataigneau et al., 1999). These findings, together with ours, lead us to conclude that vascular spheroidal endothelium stimulates SMC relaxation in response to ACh via mechanisms similar to those employed by the endothelium of ‘true’ blood vessels.

Another indication that spheroids display physiological vasodilatory responsiveness is our finding that HDL, a vasodilatory agent which acts through eNOS (Nofer et al., 2004) caused relaxation of pre-contracted spheroids. The spheroid relaxation response to HDL was also dependent on S1P3 signaling via eNOS (*data not shown*). These observations agree with findings of Noefer et al. (2004) that HDL-induced relaxation in aortic rings was dependent on S1P3 activation of eNOS.

Critical to the generation of vascular spheroids was the use of VEGF. In the absence of exogenously added VEGF, spheroids formed with a core network of small diameter blood vessels. This is in contrast to the large diameter EC-lined cavity that formed when the spheroids were cultured in VEGF-supplemented medium. Based on previous studies in which elevated VEGF levels were shown to promote the formation of large diameter vessels and vascular sinuses via the fusion of small diameter vessels (Drake and Little, 1995; Drake and Fleming, 2000; Argraves et al., 2002; Dor et al., 2002; Dominguez et al., 2007), we speculate that exogenously added VEGF acted to promote vascular fusion in the spheroids. Noteworthy in this regard is the fact that the level of serum derived VEGF in spheroid culture medium supplemented with fetal bovine serum (10% final concentration) was insufficient to promote vascular fusion.

There are several possible mechanisms by which exogenously added VEGF could induce vascular fusion (Kowanetz and Ferrara, 2006). One possibility is that exogenously added VEGF augments signaling through the low affinity VEGF receptor (Flk-1). Mechanistically, the availability of VEGF for binding to Flk-1 (K_D = 760 pmol/L) (Waltenberger et al., 1994) is limited by high affinity VEGF binding to the high affinity VEGF receptor, Flt1 (K_D = 16 pmol/L) (Hornig et al., 2000; Shibuya, 2001). In the spheroid culture, elevated VEGF levels may overcome Flt-1-mediated suppression of VEGF signaling and thereby mediate vascular fusion. This is consistent with the vascular fusion-like phenotype observed in mice lacking Flt1 (Fong et al., 1995).

The vascular spheroids described herein provide a novel tool for evaluating the role of EC-SMC interactions in the morphogenesis/maturation of embryonic blood vessels. We also demonstrate the utility of the spheroids to evaluate the significance of genetic mutation (i.e., *S1P3* knockout) on vascular tone. Vascular spheroids derived from embryos bearing targeted gene mutations may prove useful for analyzing the function(s) of genes implicated in blood vessel maturation and/or vascular tone, and particularly for those in which the mouse mutants die early in development and, thus, preclude the use of the aortic ring assay.

We also recognize the potential utility of vascular spheroids to act as modules to engineer blood vessels. This possibility is strengthened by evidence that other types of tissue spheroids can fuse. For example, spheroids generated from proepicardial tissue, which is a source of EC progenitor cells that contribute to coronary vessel formation, can fuse to form linear structures (Perez-Pomares et al., 2006). We also believe that the use of exogenous VEGF to transform networks of vessels into large vessels, as we have shown here, will be translatable to the process of engineering blood vessel-like spheroids from either adult human SMCs and ECs or from SMCs and ECs derived from stem cells.

Experimental Procedures

Reagents

Rat antibodies to mouse PECAM-1 and VE-cadherin were obtained from BD PharMingen (San Diego, CA). Rat antibodies to mouse CD34 were purchased from Research Diagnostics Inc. (Flanders, NJ). Cy3 conjugated anti-smooth muscle alpha actin (SMαA, clone 1A4) was purchased from Sigma-Aldrich (St. Louis, MO). Rabbit anti-mouse SM22-α was purchased from Abcam (Cambridge, MA) and Rabbit anti-human smooth muscle myosin II heavy chain was purchased from Biomedical Technologies, Inc. (Stoughton, MA). Fluorescently conjugated secondary antibodies were purchased from Jackson ImmunoResearch Labs, Inc. (West Grove, PA). Recombinant human $VEGF_{165}$ was obtained from R&D Systems (Minneapolis, MN). Potassium chloride (KCl), acetylcholine, N-nitro-L-arginine methyl ester/L-NAME and Hoechst 33342 nuclear stain were purchased from Sigma-Aldrich. Quantum dot 655 nanocrystals were obtained from Invitrogen (Carlsbad, California) as part of a Qtracker 655 Kit (cat. # Q25021MP). High-density lipoproteins (HDL, 1.063<d<1.21 g/ml) were isolated from the blood of normolipemic volunteers not receiving prescription medication for any acute or chronic condition and without family history of coronary artery disease, peripheral vascular disease, or stroke.

Mice

Embryonic tissues used for this study were obtained from approximately 80 wild-type ICR timed-pregnant female mice purchased from Harlan (Indianapolis, IN). Mice with a targeted deletion of the S1P3 gene (Kono et al., 2004) were obtained from Dr. Rick L. Proia (National Institutes of Health, Bethesda, Maryland). Ten timed-pregnant S1P3 null mice were used in this study.

Generation of spheroids from allantoic tissue

To generate spheroids, E8.5 mouse allantoic tissue was first isolated as previously described (Drake and Fleming, 2000; Argraves et al., 2002). Individual allantoides were then suspended in 30 μl of complete culture medium (Dulbecco's Modified Eagles Medium {DMEM, Invitrogen}) supplemented with 10% FBS (Atlanta Biologicals, Lawrenceville, GA) and 1% penicillin, streptomycin/L-glutamine (Invitrogen), and spotted onto the underside of a lid of a 60 mm plastic bacterial culture dish (Fisher Scientific, Sewanee, GA). The lids were then inverted and placed onto culture dishes to create hanging drops. The hanging drop cultures were placed in a humidified container and cultured for 18 hours (37°C, 5% CO_2). After 18 hours of culture, the resulting spheroidal-shaped tissues were resuspended in 30 μl of complete culture medium containing 0.3-1μg/ml VEGF and spotted onto the underside of a 60 mm Petri dish lid. Again, the lid was inverted, placed onto the culture dish, and the spheroids were incubated for an additional 18 hours (37°C, 5% CO_2). Spheroidal diameter measurements were made on non-fixed spheroids suspended in medium.

Fixation and immunolabeling of spheroids

Spheroids were fixed in 4% paraformaldehyde (Sigma-Aldrich; 30 minutes, 22°C) and then rinsed for 5 minutes in phosphate buffered saline containing 0.01% sodium azide (PBSA). Fixed spheroids were permeabilized in 0.02% Triton X-100/PBSA (25 minutes, 22°C), washed in PBSA, and then incubated in blocking solution (BS) containing 5% donkey serum (Jackson ImmunoResearch) and 3% bovine serum albumin (BSA, Sigma-Aldrich) in PBSA (30 minutes, 22°C). Spheroids were then incubated in primary antibodies (10μg/ml) in BS (2 hours, 22°C). Following three washes (10 minutes each, 22°C) in PBSA, spheroids were incubated in secondary antibodies (10μg/ml) in BS (2 hours, 22°C). Spheroids were then washed in PBSA (3×10 minutes, 22°C) and mounted on glass slides under number 1 cover slips (Fisher Scientific) using Gelmount mounting medium (Biomedia Corp., Foster City, CA).

Microscopic analysis of spheroids

Conventional fluorescence or differential interference contrast (DIC) images of allantoic spheroids were obtained at 22°C using a Leica DMR research grade microscope equipped with Leica objectives (5X, 10X, 20X/0.7, 40X/0.85) and a SPOT-RT camera (Vashaw Scientific, Raleigh, NC, USA). Images were acquired using SPOT-RT 3.5.7 software. Laser scanning confocal microscopic images were acquired using Zeiss 5X/0.15 and 10X/0.30 objectives on a BioRad MRC 1024 laser-scanning confocal microscope (BioRad, Microscopy Division, Cambridge, MA, USA) equipped with Lasersharp 2000 software (BioRad Cell Science Division, Hemel Hempstead, UK) or using a 20X/0.70 HC PL APO objective on a Leica TCS SP2 AOBS equipped with Leica confocal software (Leica Microsystems, Inc., Exton, PA). Confocal z-series were projected using Image J 1.31v (National Institutes of Health, USA). Montages of microscopic images were generated using Adobe Photoshop 7.0 software (Adobe Systems, Inc., San Jose, CA, USA).

Microinjection of VEGF treated spheroids

Spheroids generated in hanging drop culture were placed into a 60 mm Petri dish containing Dulbecco's phosphate buffered saline supplemented with 0.7 mmol/L $CaCl_2$ and 0.5 mmol/L $MgCl_2$ (EPBS; 22°C). The tip of a glass micropipette containing 1 ml of Qdots 655 was inserted into each spheroid and the Qdots microinjected into the central cavity using a pneumatically driven Pico-Injector (Medical Systems, Greenvale, NY). Microinjected spheroids were fixed in 4% paraformaldehyde (30 minutes, 22°C) and immunolabeled as described above.

Immunohistological analysis of spheroids

Spheroids were fixed and immunolabeled as described above, and then processed for histological analysis as follows. Spheroids were first dehydrated through a series of ethanol solutions (70%, 95%, 100%, 100%; 20 min each) and infiltrated with Histoclear II clearing solvent (National Diagnostics, Atlanta, GA) for 20 minutes (22°C). Spheroids were then infiltrated with paraffin using Histoclear:paraffin mixtures (3:1, 1:1, 1:3; 20 minutes each, 60° C), and finally infiltrated with 100% paraffin (20 minutes, 60°C). Spheroids were then embedded in paraffin and 3 μm sections were cut using a Leica RM 2125 microtome (Vashaw Scientific, Raleigh, NC), mounted on glass slides, cleared, and cover slipped for microscopic analysis.

Physiological analysis of uniluminal vascular spheroids

Spheroids were first embedded in gels composed of type I collagen. The collagen solution (1.3 mg type I collagen/ml) was prepared at 4°C by combining 0.8 ml of a 3.13 mg/ml solution of rat-tail collagen type I (BD Biosciences, Bedford, MA) with 1 ml of complete medium and 0.1 ml of sterile water (pH 7.5). A drop (80 μl) of chilled collagen solution was then pipetted onto the surface of a bacterial culture dish and individual spheroids, which had also been transferred into chilled collagen solution, were then pipetted into the drops. Following a 15-minute incubation period (37°C, 5% CO_2) to allow for polymerization of the collagen, serum-free medium was added to the cultures. The cultures were then incubated in serum-free medium containing either KCl (100 mmol/L), acetylcholine (0.001 nmol/L - 1 mmol/L), L-NAME (3 mmol/L) or HDL (500 mg/ml). Following addition of each agent, sequential images of the spheroids were acquired using a Leica MZ-12 microscope equipped with a Dage MTI CDD-300 camera. Morphometric measurements (diameter) were made from the images using Image J 1.31v software (National Institutes of Health, USA). The percentage of the maximal possible spheroid relaxation induced by HDL was calculated as the quotient of Δ1 (the diameter of HDL treated spheroid-1 minus its KCl-contracted diameter) and Δ2 (the diameter of untreated spheroid-1 minus its KCl-contracted diameter) × 100.

Acknowledgments

The authors thank Dr. Tim McQuinn for advice and critical suggestions, and Joyce Edmunds for assistance with histology. We also thank Dr. Richard L. Proia (National Institutes of Health, Bethesda, MD) for providing us with the mouse strain carrying a targeted deletion of the S1P3 gene and Dr. Samar M. Hammad (Medical University of South Carolina) for providing us with HDL.

Grant information: NIH HL57375 and NIH HL80168 (CJD); NIH HL061873 (WSA); NIH HL080404 (KMA), NSF FIBR-0526854 (VM).

References

Argraves WS, Larue AC, Fleming PA, Drake CJ. VEGF signaling is required for the assembly but not the maintenance of embryonic blood vessels. Dev Dyn 2002;225:298–304. [PubMed: 12412012]

Chataigneau T, Feletou M, Huang PL, Fishman MC, Duhault J, Vanhoutte PM. Acetylcholine-induced relaxation in blood vessels from endothelial nitric oxide synthase knockout mice. Br J Pharmacol 1999;126:219–226. [PubMed: 10051139]

Dominguez MG, Hughes VC, Pan L, Simmons M, Daly C, Anderson K, Noguera-Troise I, Murphy AJ, Valenzuela DM, Davis S, Thurston G, Yancopoulos GD, Gale NW. Vascular endothelial tyrosine phosphatase (VE-PTP)-null mice undergo vasculogenesis but die embryonically because of defects in angiogenesis. Proc Natl Acad Sci U S A 2007;104:3243–3248. [PubMed: 17360632]

Dor Y, Djonov V, Abramovitch R, Itin A, Fishman GI, Carmeliet P, Goelman G, Keshet E. Conditional switching of VEGF provides new insights into adult neovascularization and pro-angiogenic therapy. Embo J 2002;21:1939–1947. [PubMed: 11953313]

Dora KA, Doyle MP, Duling BR. Elevation of intracellular calcium in smooth muscle causes endothelial cell generation of NO in arterioles. Proc Natl Acad Sci U S A 1997;94:6529–6534. [PubMed: 9177252]

Downs KM, Temkin R, Gifford S, McHugh J. Study of the murine allantois by allantoic explants. Dev Biol 2001;233:347–364. [PubMed: 11336500]

Drake CJ, Fleming PA. Vasculogenesis in the day 6.5 to 9.5 mouse embryo. Blood 2000;95:1671–1679. [PubMed: 10688823]

Drake CJ, Little CD. Exogenous vascular endothelial growth factor induces malformed and hyperfused vessels during embryonic neovascularization. Proc Natl Acad Sci U S A 1995;92:7657–7661. [PubMed: 7543999]

Duband JL, Gimona M, Scatena M, Sartore S, Small JV. Calponin and SM 22 as differentiation markers of smooth muscle: spatiotemporal distribution during avian embryonic development. Differentiation 1993;55:1–11. [PubMed: 8299876]

Fong GH, Rossant J, Gertsenstein M, Breitman ML. Role of the Flt-1 receptor tyrosine kinase in regulating the assembly of vascular endothelium. Nature 1995;376:66–70. [PubMed: 7596436]

Frid MG, Kale VA, Stenmark KR. Mature vascular endothelium can give rise to smooth muscle cells via endothelial-mesenchymal transdifferentiation: in vitro analysis. Circ Res 2002;90:1189–1196. [PubMed: 12065322]

Furchgott RF, Zawadzki JV. The obligatory role of endothelial cells in the relaxation of arterial smooth muscle by acetylcholine. Nature 1980;288:373–376. [PubMed: 6253831]

Hadoke PW, Christy C, Kotelevtsev YV, Williams BC, Kenyon CJ, Seckl JR, Mullins JJ, Walker BR. Endothelial cell dysfunction in mice after transgenic knockout of type 2, but not type 1, 11beta-hydroxysteroid dehydrogenase. Circulation 2001;104:2832–2837. [PubMed: 11733403]

Hornig C, Barleon B, Ahmad S, Vuorela P, Ahmed A, Weich HA. Release and complex formation of soluble VEGFR-1 from endothelial cells and biological fluids. Lab Invest 2000;80:443–454. [PubMed: 10780661]

Ishisaki A, Hayashi H, Li AJ, Imamura T. Human umbilical vein endothelium-derived cells retain potential to differentiate into smooth muscle-like cells. J Biol Chem 2003;278:1303–1309. [PubMed: 12417591]

Kelm JM, Diaz Sanchez-Bustamante C, Ehler E, Hoerstrup SP, Djonov V, Ittner L, Fussenegger M. VEGF profiling and angiogenesis in human microtissues. J Biotechnol 2005;118:213–229. [PubMed: 15951040]

Kono M, Mi Y, Liu Y, Sasaki T, Allende ML, Wu YP, Yamashita T, Proia RL. The sphingosine-1-phosphate receptors S1P1, S1P2, and S1P3 function coordinately during embryonic angiogenesis. J Biol Chem 2004;279:29367–29373. [PubMed: 15138255]

Korff T, Kimmina S, Martiny-Baron G, Augustin HG. Blood vessel maturation in a 3-dimensional spheroidal coculture model: direct contact with smooth muscle cells regulates endothelial cell quiescence and abrogates VEGF responsiveness. Faseb J 2001;15:447–457. [PubMed: 11156960]

Kowanetz M, Ferrara N. Vascular endothelial growth factor signaling pathways: therapeutic perspective. Clin Cancer Res 2006;12:5018–5022. [PubMed: 16951216]

Li L, Miano JM, Cserjesi P, Olson EN. SM22 alpha, a marker of adult smooth muscle, is expressed in multiple myogenic lineages during embryogenesis. Circ Res 1996;78:188–195. [PubMed: 8575061]

Madsen CS, Regan CP, Hungerford JE, White SL, Manabe I, Owens GK. Smooth muscle-specific expression of the smooth muscle myosin heavy chain gene in transgenic mice requires 5′-flanking and first intronic DNA sequence. Circ Res 1998;82:908–917. [PubMed: 9576110]

Miano JM, Cserjesi P, Ligon KL, Periasamy M, Olson EN. Smooth muscle myosin heavy chain exclusively marks the smooth muscle lineage during mouse embryogenesis. Circ Res 1994;75:803–812. [PubMed: 7923625]

Murata N, Sato K, Kon J, Tomura H, Yanagita M, Kuwabara A, Ui M, Okajima F. Interaction of sphingosine 1-phosphate with plasma components, including lipoproteins, regulates the lipid receptor-mediated actions. Biochem J 2000;352(Pt 3):809–815. [PubMed: 11104690]

Nofer JR, van der Giet M, Tolle M, Wolinska I, von Wnuck Lipinski K, Baba HA, Tietge UJ, Godecke A, Ishii I, Kleuser B, Schafers M, Fobker M, Zidek W, Assmann G, Chun J, Levkau B. HDL induces NO-dependent vasorelaxation via the lysophospholipid receptor S1P3. J Clin Invest 2004;113:569–581. [PubMed: 14966566]

Perez-Pomares JM, Mironov V, Guadix JA, Macias D, Markwald RR, Munoz-Chapuli R. In vitro self-assembly of proepicardial cell aggregates: an embryonic vasculogenic model for vascular tissue engineering. Anat Rec A Discov Mol Cell Evol Biol 2006;288:700–713. [PubMed: 16761281]

Rieger S, Kulkarni RP, Darcy D, Fraser SE, Koster RW. Quantum dots are powerful multipurpose vital labeling agents in zebrafish embryos. Dev Dyn 2005;234:670–681. [PubMed: 16110511]

Rohrer L, Cavelier C, Fuchs S, Schluter MA, Volker W, von Eckardstein A. Binding, internalization and transport of apolipoprotein A-I by vascular endothelial cells. Biochim Biophys Acta 2006;1761:186–194. [PubMed: 16546443]

Ross JJ, Hong Z, Willenbring B, Zeng L, Isenberg B, Lee EH, Reyes M, Keirstead SA, Weir EK, Tranquillo RT, Verfaillie CM. Cytokine-induced differentiation of multipotent adult progenitor cells into functional smooth muscle cells. J Clin Invest 2006;116:3139–3149. [PubMed: 17099777]

Scharpfenecker M, Fiedler U, Reiss Y, Augustin HG. The Tie-2 ligand angiopoietin-2 destabilizes quiescent endothelium through an internal autocrine loop mechanism. J Cell Sci 2005;118:771–780. [PubMed: 15687104]

Shibuya M. Structure and dual function of vascular endothelial growth factor receptor-1 (Flt-1). Int J Biochem Cell Biol 2001;33:409–420. [PubMed: 11312109]

Teerlink T, Scheffer PG. LDL particles are nonspherical: consequences for size determination and phenotypic classification. Clin Chem 2007;53:361–362. [PubMed: 17259250]

Waltenberger J, Claesson-Welsh L, Siegbahn A, Shibuya M, Heldin CH. Different signal transduction properties of KDR and Flt1, two receptors for vascular endothelial growth factor. J Biol Chem 1994;269:26988–26995. [PubMed: 7929439]

Yamashita J, Itoh H, Hirashima M, Ogawa M, Nishikawa S, Yurugi T, Naito M, Nakao K. Flk1-positive cells derived from embryonic stem cells serve as vascular progenitors. Nature 2000;408:92–96. [PubMed: 11081514]

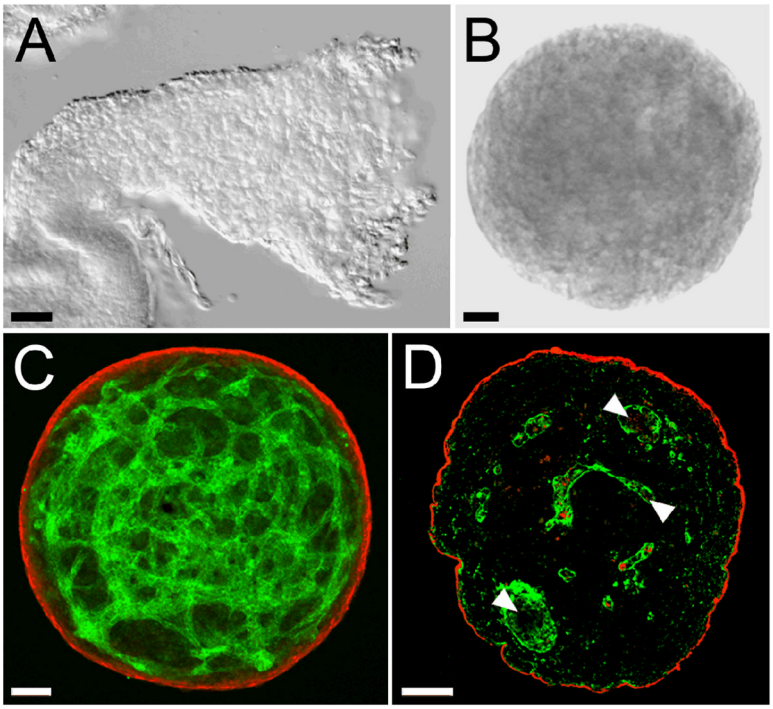

Figure 1. Spheroids produced by hanging drop culture of allantoic tissue

A, DIC image of an isolated allantois from an E8.5 embryo. ***B***, DIC image of a spheroid generated by incubation of E8.5 allantoic tissue for 18 hours in hanging drop culture. ***C***, LSCM image of an allantoic-derived spheroid immunolabeled with antibodies to PECAM-1 (*green*) and SMαA (*red*). The data presented in C is representative of microscopic analysis of >10 spheroids. ***D***, Epifluorescence microscopic image of a 3 μm section of a paraffin embedded allantoic-derived spheroid immunolabeled with antibodies to PECAM-1 (*green*) and SMαA (*red*). *Arrowheads* in D point to immunonegative areas that may represent either lumens within capillary-like blood vessels or extravascular spaces. The data presented in D is representative of microscopic analysis of two spheroids. Bars equal 50 μm.

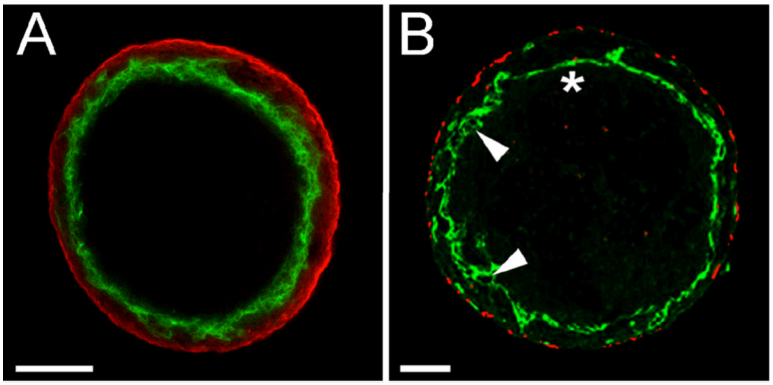

Figure 2. VEGF promotes the fusion of the capillary-like vessels present in allantoic-derived spheroids

A, A single optical section acquired from the middle of a VEGF treated spheroid immunolabeled with antibodies to PECAM-1 (*green*) and SMαA (*red*) depicts a single inner layer of PECAM-1 positive cells surrounding a central immuno-negative cavity. The data presented in A is representative of microscopic analysis of >10 spheroids. ***B***, epifluorescence image of a 3 μm physical section of a VEGF treated spheroid immunolabeled with antibodies to PECAM-1 (*green*) and SMαA (*red*). *Asterisk* indicates a squamous portion of the endothelium while *arrowheads* indicate more stratified portions of the endothelium. The data presented in B is representative of microscopic analysis of two spheroids. Bars in *A*, *B* and *D* equal 100 μm. Bar in C equals 50 μm.

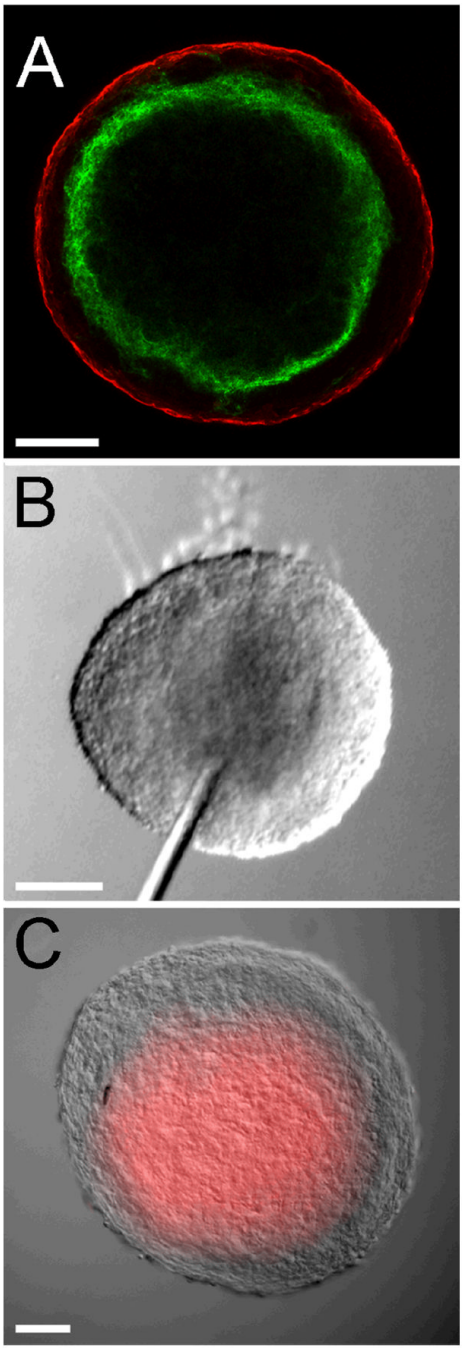

Figure 3. ECs circumscribing the central space of VEGF treated allantoic spheroid exhibit properties of an endothelium

A, LSCM optical section (3 μm) of a VEGF treated spheroid immunolabeled with antibodies to VE-cadherin (*green*) and SMαA (*red*). The data presented in A is representative of microscopic analysis of 4 spheroids. ***B*** and ***C***, DIC images of a VEGF treated spheroid prior to (*B*) and following (*C*) injection of fluorescently conjugated Qdots into the central cavity. The increment of time between the image shown (*B*) and *(C)* is <1 second. Bars equal 100 μm. The data presented in B and C is representative of microscopic analysis of 6 spheroids.

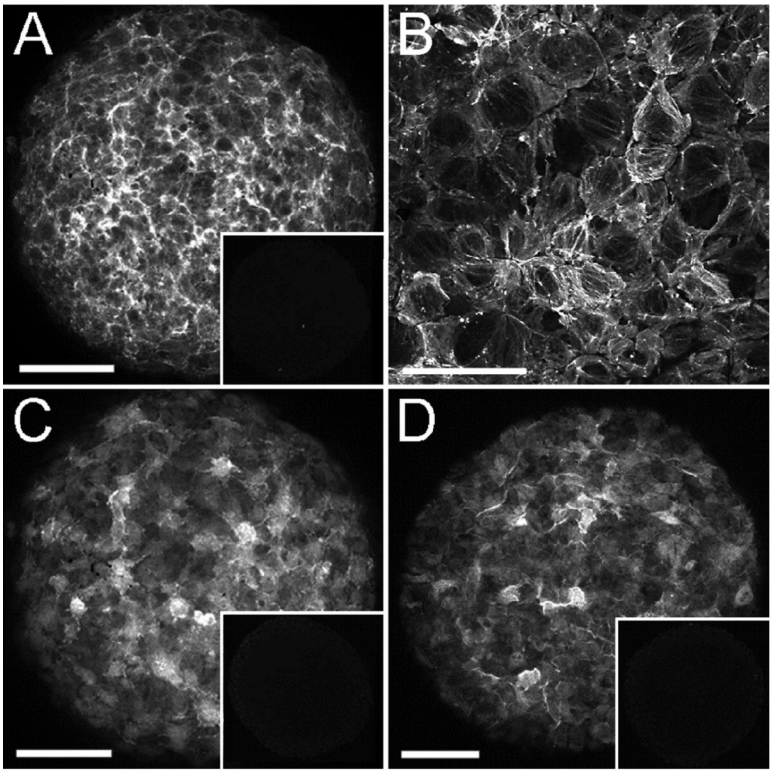

Figure 4. Cells of the outer layer of spheroids express SMC proteins

A, C and ***D***, LSCM collapsed z-series of VEGF-treated spheroids immunolabeled with antibodies to SMαA (***A***), SM22-α (***C***) and SM-MHC (***D***). *Insets* in A, C and D show immunostaining obtained using control IgG of the same isotype used in the respective panel. ***B*** shows SMαA-positive intracellular fibers in a high magnification view of VEGF-treated spheroids. Bars in *A*, *C* and *D* equal 100 μm. Bar in B equals 50 μm. The data presented is representative of confocal analysis of >6 spheroids stained with each antibody.

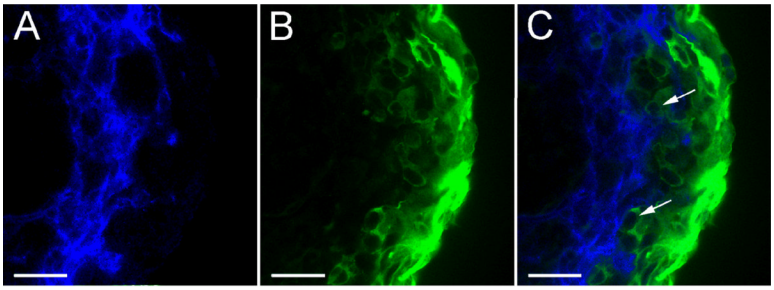

Figure 5. SM22-α-positive cells are positioned immediately adjacent to ECs

A-C show a single 3 μm optical cross section from the center of a VEGF-treated spheroid double labeled with antibodies to PECAM-1 (*blue*) and SM22-α (*green*). ***A***, anti-PECAM-1 immunolabeling. ***B***, anti-SM22-α immunolabeling. ***C***, merged anti-PECAM-1 and anti-SM22-α immunolabeling. Bars equal 50μm. The data presented is representative of confocal analysis of >6 spheroids stained with each antibody.

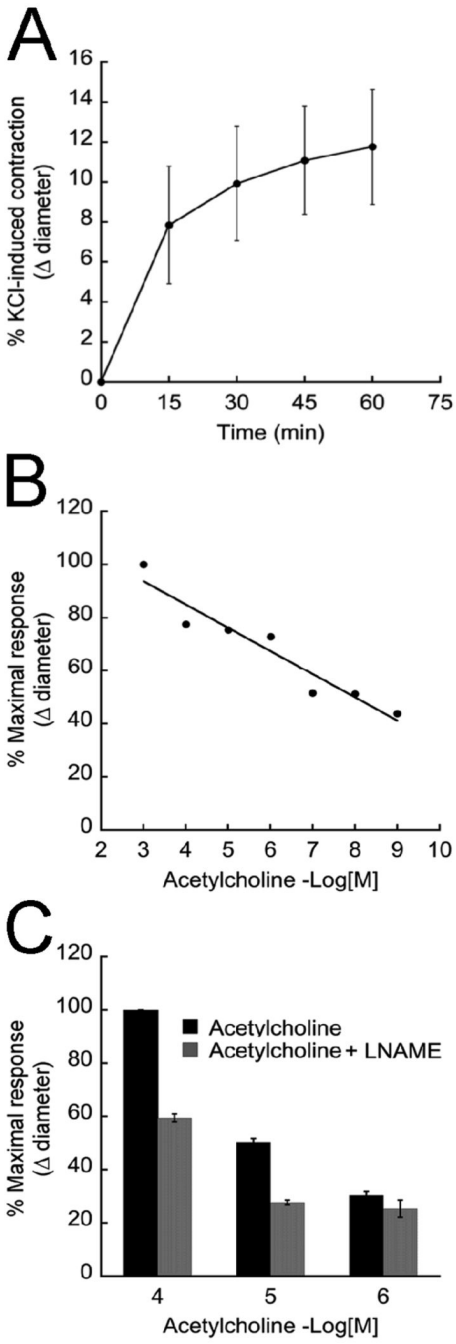

Figure 6. Uniluminal vascular spheroids respond to vasoactive compounds

A, KCl treatment of VEGF-treated spheroids causes a time-dependent reduction in spheroid diameter. Each plotted value represents the percent change in diameter ± StDv as a function of the amount of time that spheroids (n=13) were exposed to KCl. The data presented in A is representative of 3 experiments. ***B***, KCl-treated vascular spheroids show a concentration-dependent increase in diameter ± StDv (vasorelaxation) in response to acetylcholine treatment (0.001 nmol/L - 1 mmol/L, n=3). The data presented in B is representative of 2 experiments. ***C***, the effect of L-NAME (3 mmol/L) on acetylcholine-mediated vasorelaxation ($p<0.01$) of KCl-treated spheroids (n=3). Plotted values in C represents the percent change in diameter ± StDv. The data presented in C is representative of 2 experiments.

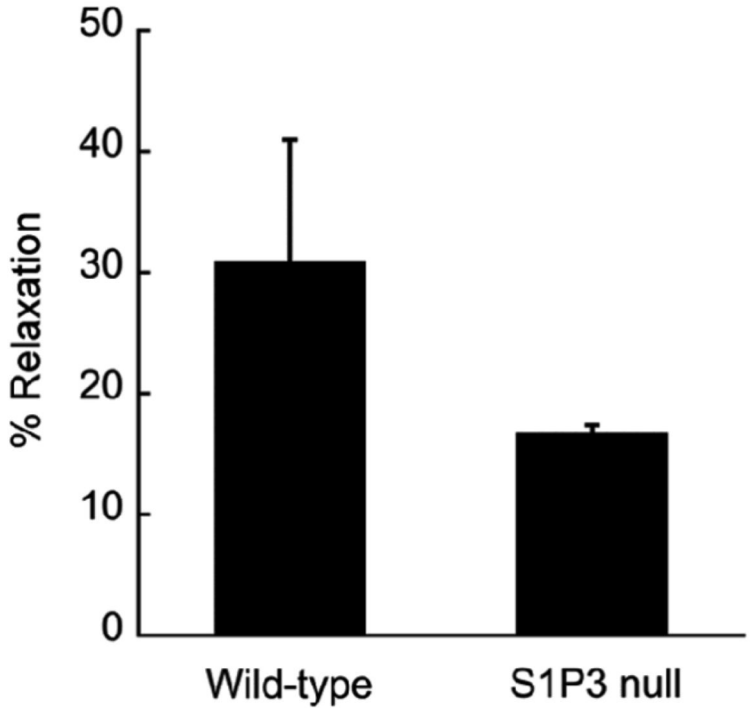

Figure 7. HDL induces vasorelaxation of spheroids

Spheroids derived from wild-type and S1P3 null embryos were pre-contracted with KCl and then treated with HDL (500 μg/ml) for 2 hours. The plotted values represent the percent of maximal spheroid relaxation (as a function of change in spheroid diameter) achieved in response to HDL treatment (wild-type n =4; null n = 2). The data presented is representative of 2 experiments.